Article

Oxidative Alcohol Dehydrogenation with Small Size of Cobalt Oxide Catalyst Derived from Activated Al_2O_3-supported Co^{2+}-Al^{3+} Layered Double Hydroxide

Febi Yusniyanti [1], Takayoshi Hara [1]*, Tomohiko Okada [2], Takuya Fujimura [3], Ryo Sasai [3], Chikako Moriyoshi [4], Shogo Kawaguchi [5] and Nobuyuki Ichikuini [1]

[1] Department of Applied Chemistry and Biotechnology, Graduate School of Engineering, Chiba University, 1-33 Yayoi, Inage, Chiba, 263-8522, Japan

[2] Department of Materials Chemistry, Faculty of Engineering, Shinshu University, 4-17-1 Wakasato, Nagano, Nagano 380-8553, Japan

[3] Graduate School of Natural Science and Technology, Shimane University, 1060 Nishi-Kawatsu, Matsue, Shimane 690-8504, Japan

[4] Graduate School of Advanced Science and Engineering, Hiroshima University, 1-3-1 Kagamiyama, Higashi-Hiroshima, Hiroshima 739-8526, Japan

[5] Japan Synchrotron Radiation Research Institute (JASRI), 1-1-1 Kouto, Sayo-cho, Sayo-gun, Hyogo 679-5198, Japan

* Corresponding author: t_hara@faculty.chiba-u.jp

Abstract

The carbonate-intercalated Co^{2+}-Al^{3+} layered double hydroxide (CO_3^{2-}/CoAl LDH) supported on activated alumina, denoted as Al_2O_3, was successfully synthesized through the coprecipitation method. The resulting X-ray diffraction profiles confirmed the formation of CO_3^{2-}/CoAl LDH@Al_2O_3, illustrating the integration of the LDH structure with the support material. Upon calcination at 573 K under air, the LDH structure underwent collapse, as evidenced by temperature-programmed synchrotron XRD and thermogravimetric-differential thermal analysis, leading to the generation of Co_3O_4 nanoparticles, as indicated by Co K-edge X-ray absorption near-edge structure spectra. When employed as a catalyst in the oxidative dehydrogenation of 1-phenyl ethanol with molecular oxygen as the oxidant, our synthesized catalyst exhibited superior catalytic activity, achieving a turnover number value of 10.6, thus highlighting its potential in the catalytic process.

Keywords: Co^{2+}-Al^{3+} layered double hydroxide, Co_3O_4 supported on Al_2O_3, Calcination, Aerobic alcohol oxidation,

1. Introduction

Layered double hydroxide (LDH), also known as anionic clay or hydrotalcite like materials, is layered material consisting of mixed of divalent and trivalent metal cations binding together with edge sharing as a main layer structure similar to that of brucite materials and anion in the interlayer space balancing the charge. The general formula of LDH is given as $[M(II)_{1-x}M(III)_x(OH)_2]^{x+}(A^{n-}_{x/n})\cdot mH_2O$, where M(II) and M(III) represented divalent and trivalent metal cation respectively, and A^{n-} is inorganic or organic anion filling the interlayer space[1–3]. Various kinds of divalent metal cations can be introduced into the layer structure of LDH to make the versatile application of LDH as a catalyst[4–6] or an adsorbent[7,8]. Many reports mentioned that catalyst based LDH could be used as a catalyst for wide organic transformation. In addition to that, metal oxide obtained from the calcination of LDH precursor exhibited excellent catalytic activity

compared to commercially available and other synthesis methods[9,10]. It brings to light that LDH as a catalyst precursor is desired.

Transition metal oxide is a promising catalyst to replace precious metal catalyst to have reported exhibiting good catalytic performance[11–13]. However, transition metal oxide usually possessed a big particle size and small surface area limiting their application as a catalyst. Therefore, creating metal oxide with excellent properties is a challenging task. To overcome that challenge, various synthesis routes in obtaining transition metal oxide have been developed to modify their properties and catalytic performance[14–16]. It was reported that transition metal oxide-based catalyst can be prepared from LDH precursor after calcination at desired temperature. It has large surface area, good thermal stability, good metal dispersion and unique reduction behavior, which is suitable to be applied as a catalyst[9,10,17].

Oxidation of alcohol is one of the crucial organic reactions to produce aldehyde which is an important intermediate in pharmaceuticals. The oxidative alcohol dehydrogenation employed oxidants such as *tert*-butyl hydroperoxide (TBHP)[4,18–20], hydrogen peroxide (H_2O_2)[21–23], air[24–26] and molecular oxygen (O_2)[27–30]. In recent years, O_2 has gained attention as an oxidant because it is a more environmentally friendly route as it releases water as the only byproduct. However, finding a suitable catalyst to utilize molecular oxygen as an oxidant is one of the great challenges. Among the available transition metal-based catalysts, Co_3O_4 is highly active for oxidative alcohol dehydrogenation using molecular oxygen as an oxidant. Furthermore, Co_3O_4 in nanosized exhibited higher activity compared to the bulk one because there are more catalytically active sites available for the reaction to proceed[29]. To create nanosized Co_3O_4, transition metal oxide precursor is deposited onto the support materials such as, alumina[31], MnO_2[32], and SBA-15[33].

Many reports have also shown that LDH nanosized can be created by constructing LDH on the surface of support material. Previously, we successfully synthesized CuAl LDH@α-Al_2O_3 by simple coprecipitation of metal precursor in the presence of Al_2O_3 as support; followed by the calcination at 1073 K, CuAlO@α-Al_2O_3 exhibited excellent catalytic activity towards acceptorless dehydrogenation of various alcohols[34]. In this report, the Co_3O_4 supported on activated Al_2O_3, Co_3AlO_x@Al_2O_3, was synthesized via the carbonate-intercalated Co^{2+}-Al^{3+} layered double hydroxide (CO_3^{2-}/Co_3Al LDH) precursor supported on activated Al_2O_3 by coprecipitation method followed by calcination at 537 K. The different Co-loading amounts were investigated on their catalytic activity of aerobic alcohol oxidation using 1-phenyl ethanol as a model. X-ray diffraction (XRD), temperature programmed synchrotron X-ray diffraction (*tp*-SXRD), thermogravimetric-differential thermal analysis (TG-DTA), and Co K-edge X-ray absorption near edge structure (XANES) were used to elucidate the structure of the catalyst.

2. Experimental

2.1 Catalyst preparation

The CO_3^{2-}/Co_3Al LDH was supported on activated Al_2O_3 (denoted as Al_2O_3, purchased from FUJIFILM Wako Pure Chemical Corporation) through the direct coprecipitation in the presence of Al_2O_3 under the alkaline condition following the previous report with some modifications[35,36]. The mixture of Co^{2+} and Al^{3+} (Co/Al molar ratio = 3) was prepared by dissolving $Co(NO_3)_2{\cdot}6H_2O$ (3 mmol) and $Al(NO_3)_3{\cdot}9H_2O$ (1 mmol) in 50 mL of Milli-Q water. The mixture was slowly added using peristaltic pump into the mixture of 100 mL of Na_2CO_3 (45 mmol/L) and 3 g of Al_2O_3 at room temperature under a constant stirring. The pH of mixture was controlled approximately at 9.5 by adding aqueous NaOH (1 mol/L). Afterward, the resulted slurry was heated at 333 K for an hour. The obtained pink suspension was cooled down, filtered, washed with water, and dried at 333 K overnight to obtain 0.91_CO_3^{2-}/Co_3Al LDH@Al_2O_3. The Co loading amount in the 0.91_CO_3^{2-}/Co_3Al LDH@Al_2O_3 was calculated at 0.91 mmol/g, confirmed by atomic absorption spectroscopy (AAS) using Thermo Elemental SOLLAR S4 flame atomic-absorption spectrometer equipped with a cobalt hollow cathode lamp (240.73 nm, Hamamatsu photonics K.K.), atomizing by air-acetylene flame as follows; the weight-measured solid catalyst was dissolved in hot nitric acid and diluted, and remained solid Al_2O_3 was separated by a simple centrifugation before measurement of AAS. The 0.91_CO_3^{2-}/Co_3Al LDH@Al_2O_3 was calcined at 573 K for 2 h (heating rate was 10 K/min) under air flow (flow rate was 3 L/min) and denoted as 0.98_Co_3AlO_x@Al_2O_3. The Co content in the 0.98_Co_3AlO_x@Al_2O_3 was determined to be 0.98 mmol/g by AAS. The 0.98_Co@Al_2O_3_Imp catalyst was also synthesized via a simple impregnation method: stirring 2.94 mmol $Co(NO_3)_2{\cdot}6H_2O$ and 3 g of Al_2O_3 in 100 mL of distillated water, continue with evaporation and calcination at 573 K for 2 h. For comparison, 2.50 and 1.41 mmol/g Co of CO_3^{2-}/Co_3Al LDH supported on Al_2O_3 was prepared by the similar procedure as 0.91_CO_3^{2-}/Co_3Al LDH@Al_2O_3 by changing the support amount from 3 g to 1 and 2 g, respectively for 2.50_CO_3^{2-}/Co_3Al LDH@Al_2O_3 and 1.41_CO_3^{2-}/Co_3Al LDH@Al_2O_3. The Co content in the calcined Co_3AlO_x@Al_2O_3 derived from 2.50_CO_3^{2-}/Co_3Al LDH@Al_2O_3 and 1.41_CO_3^{2-}/Co_3Al LDH@Al_2O_3 were also determined by AAS to 2.87 mmol/g (2.87_Co_3AlO_x@Al_2O_3) and 1.59 mmol/g (1.59_Co_3AlO_x@Al_2O_3), respectively. Unsupported CO_3^{2-}/Co_3Al LDH was also prepared using a similar method without the addition of Al_2O_3. The Co_3AlO_x catalyst was prepared by the same calcination of CO_3^{2-}/Co_3Al LDH. The Co content in the CO_3^{2-}/Co_3Al LDH and Co_3AlO_x was 8.59 and 9.33 mmol/g.

2.2 Catalyst characterization

XRD was performed on the Rigaku MiniFlex 600 using monochromatic Cu Kα radiation (λ = 0.15418 nm) generated at 40 kV and 15 mA and collected with D/teX Ultra 250 1D detector recorded at 2θ of 5 to 80 deg with divergence slit of 0.625°, scattering slit of 1.25°, receiving slit of 0.30 mm, step width of 0.02°, and the scan speed of 10 deg/min. A *tp*-SXRD profile was collected at BL02B2 of SPring-8 using multiple MYTHEN detector. The X-ray wavelength with 0.078 nm (15.5 keV) was used for this experiment. Homogeneous granularity powder of 0.91_CO_3^{2-}/Co_3Al LDH@Al_2O_3 was sealed in a quartz capillary with an internal diameter of 0.3 mm. The sample was heated proportionally in an electric furnace (10 K/min), and the synchrotron XRD profiles were chalked up every 10 s. Cobalt K-edge XANES spectra were recorded at room temperature in a transmission mode at the facilities installed on the BL-12C station of Photon Factory attached with a Si–(111) double crystal monochromator. Data analysis was carried out with the Athena XAS data processing program[37]. TG-DTA was carried out using Rigaku thermoplus EVO II TG-DTA TG28120 starting from ambient temperature to 1173 K (heating rate: 10 K/min) under air flow. Catalytic activity was determined using gas chromatography (GC) with a flame ionization detector (FID) equipped with a Shimadzu CPB20 wide-bore capillary column; length: 25 m, internal diameter: 0.53 mm, and film thickness: 1 µm. The injector temperature was 493 K, while the initial and the final temperature were 353 K and 473 K, respectively, with a 16 K/min heating rate.

2.3 Catalytic activity test

Prepared catalysts were tested on the oxidative dehydrogenation of 1-phenyl ethanol. Typically, 1-phenyl ethanol (1 mmol), catalyst (0.05 g), and mesitylene (3 mL) as a solvent were loaded into the Schlenk tube and connected with a condenser. Molecular oxygen (0.1 MPa) was introduced into the reactor using a balloon. The reaction was carried out at 433 K for 2 h. The reaction mixture was collected and separated from catalyst using centrifugation. Afterward, the reaction mixture in the liquid phase was analyzed by GC using an internal standard technique to determine the conversion based on 1-phenyl ethanol, the yield, and the selectivity of acetophenone.

3. Results and Discussion

3.1 Catalyst preparation and characterization

The XRD analysis was conducted to confirm the formation of LDH on the support and was compared with the unsupported CO_3^{2-}/Co_3Al LDH, presented in **Fig. 1**. Unsupported CO_3^{2-}/Co_3Al LDH exhibited a typical XRD profile of the hydrotalcite-like layered materials. Peaks attributed to LDH appeared at 2θ of 11.3°, 23.2°, 34.4°, 59.2° and 60.4° which corresponded to (003), (006), (012), (110), and (113) lattice planes (**Fig. 1(a)**). No other impurities were found in the XRD profile. Similar peaks were found in the XRD profile of 0.91_CO_3^{2-}/Co_3Al LDH@Al_2O_3. Other peaks assigned to Al_2O_3 at 2θ = 14.5°, 28.2°, 38.3°, 42.5°, 45.4°, 48.9°, and 67.2° accompanied the LDH's peaks were observed in **Figs. 1(b)-(d)**.

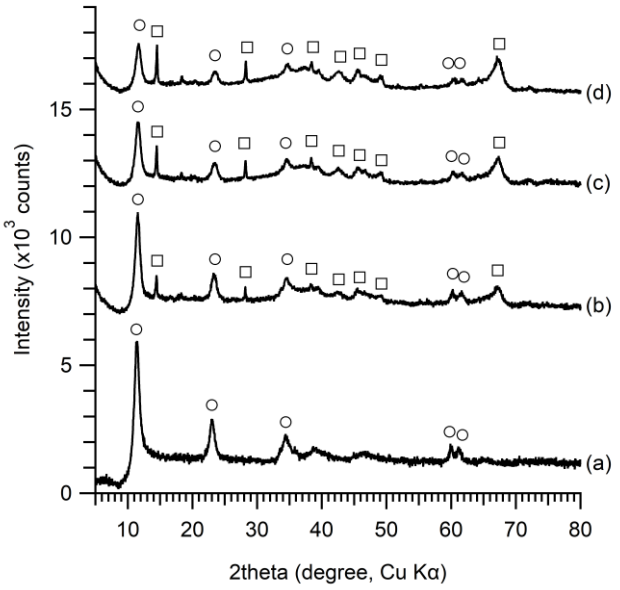

Fig. 1 XRD profiles for (a) CO_3^{2-}/Co_3Al LDH, (b) 2.50_CO_3^{2-}/Co_3Al LDH@Al_2O_3, (c) 1.41_CO_3^{2-}/Co_3Al LDH@Al_2O_3, (d) 0.91_ CO_3^{2-}/Co_3Al LDH@Al_2O_3. (○: LDH, □: Al_2O_3)

It was noticed that as the cobalt amount decreased, the relative peak intensity of LDH to that of Al_2O_3 decreased. The basal spacing of the (003) lattice plane (d_{003}) of the unsupported CO_3^{2-}/Co_3Al LDH was calculated to 0.779 nm using Bragg's equation, $2d\sin\theta = n\lambda$. In the case of the supported Co_3Al LDH, the d_{003} values were 0.768, 0.765, and 0.758 nm for 2.50, 1.41, and 0.91_CO_3^{2-}/Co_3Al LDH@Al_2O_3, respectively. We previously reported that cobalt-aluminum LDH with different Co/Al molar ratios had different values of d_{003}; as the Co/Al molar ratio increased, the d_{003} value increased[36]. The change of the d_{003} value of supported LDH close to the cobalt-aluminum LDH with the ratio of 2 assumed due to the Al_2O_3 as the support was partially involved in forming of lamellar structure of LDH[38,39].

Metal oxide can be obtained by simple calcination of LDH precursor accordant with the M^{2+} in the LDH structure[40,41]. **Figure 2(a)** showed the XRD profiles of CO_3^{2-}/Co_3Al LDH after calcination at 573 K (Co_3AlO_x). The calcination of the LDH precursor under air caused the formation of metal oxide. It is well known that XRD profile of Co_3O_4 is similar to that of $CoAl_2O_4$[42]. Thus, it is hard to determine if the peaks belong to Co_3O_4 or $CoAl_2O_4$ using XRD. As confirmed later by Co K-edge XANES analysis, $CoAl_2O_4$ phase did not generate during this synthetic protocol of catalyst. It is noticed that the layered structure of LDH diminished, and the peaks corresponding to the Co_3O_4 appeared at 2θ of 31.7° (220), 37.0° (311), and 45.0° (400). It confirmed that

Co_3AlO_x consists of Co_3O_4 with the crystallite size of 4.59 nm calculated using the Debye-Scherrer equation based on the (311) diffraction. The XRD profiles of Co_3AlO_x@Al_2O_3 are also displayed in **Figs. 2(b)-(d)**. The peaks of Co_3O_4 in Co_3AlO_x@Al_2O_3 can be hardly distinguished from Al_2O_3 at 2θ of 36-38°. It might be said that the highly dispersed and small size of Co_3O_4 species was formed after calcination at 573 K on the surface of Al_2O_3.

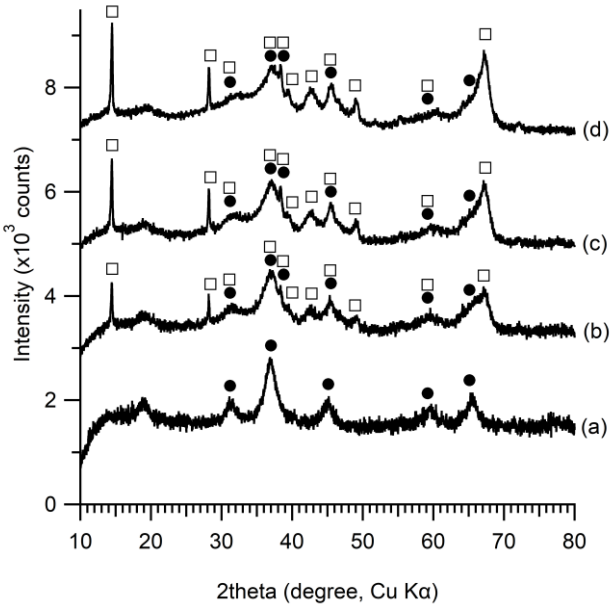

Fig. 2 XRD profiles for (a) Co_3AlO_x, (b) 2.87_Co_3AlO_x@Al_2O_3, (c) 1.59_Co_3AlO_x@Al_2O_3, and (d) 0.98_Co_3AlO_x@Al_2O_3. (●: Co_3O_4, □: Al_2O_3)

To elucidate the structural change of the 0.91_CO_3^{2-}/Co_3Al LDH@Al_2O_3 during the calcination process, in-situ *tp*-SXRD analysis was performed, and the result is displayed in **Fig. 3**. In addition, TG-DTA data, obtained by the same heating rate, was combined in the *tp*-SXRD graph. In Fig. 3, strong and sharp peak based on Al_2O_3 was observed at 7.3°. It observed the peak assigned to the LDH around 5.9° started to collapse at 423 K and completely disappeared at 548 K. The collapse in the LDH layered structure was accompanied by the weight loss in the TG-DTA profile. The first weight loss with endothermic reaction started to occur at 353 K to 403 K corresponding to the loss of the physically adsorbed water in the external structure of LDH[5,39]. The second stage of weight loss with an endothermic peak around 453 K was caused by the removal of interlayer water and intercalated carbonate ion. The dihydroxylation of the hydroxyl groups in the cationic nanosheet of LDH structure took place from 504 K to 543 K[43,44]. This stage was the main cause for the collapse of the layered structure as shown in **Fig. 3**. These findings suggested that the layered structure completely vanished after the calcination at 573 K.

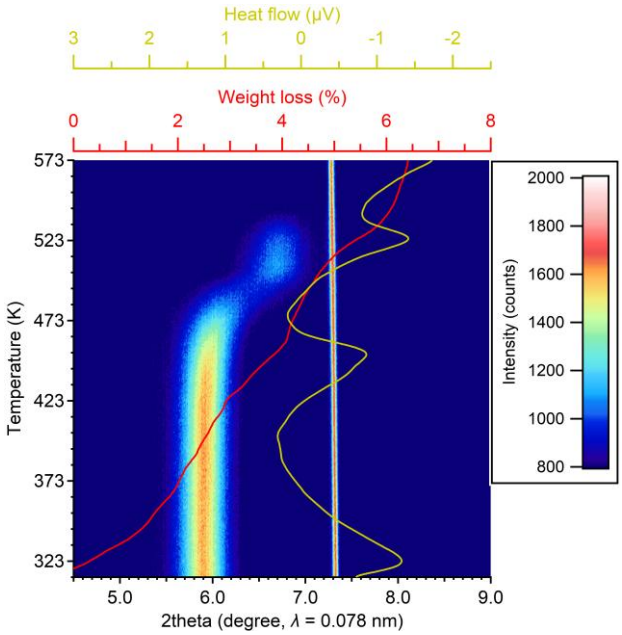

Fig. 3 2D mapping of the in-situ *tp*-SXRD profile (λ = 0.078 nm) of 0.91_Co_3Al LDH@Al_2O_3 (heating rate: 10 K/min) combined with the TG-DTA data.

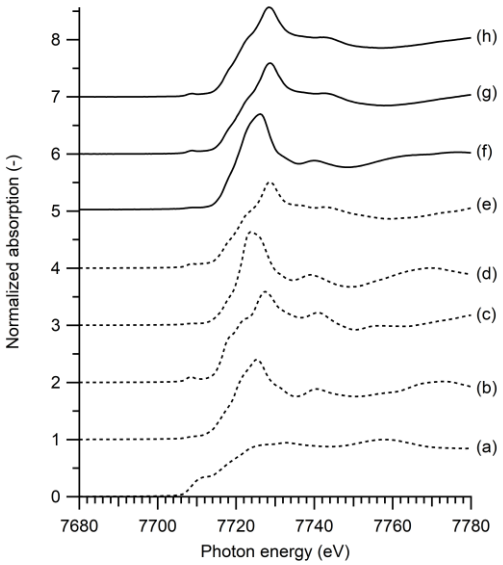

Fig. 4 Co K-edge spectra of (a) Co foil, (b) CoO, (c) $CoAl_2O_4$, (d) $Co(OH)_2$, (e) Co_3O_4, (f) 0.91_CO_3^{2-}/Co_3Al LDH@Al_2O_3, (g) 0.98_Co_3AlO_x@Al_2O_3, and (h) recovered 0.98_Co_3AlO_x@Al_2O_3 catalyst.

The cobalt species composition in the LDH precursor and oxide form after the calcination at 573 K was further investigated using Co K-edge XANES (**Fig. 4**). The peak shape of the parents 0.91_CO_3^{2-}/Co_3Al LDH@Al_2O_3 did not resemble to Co foil, CoO, $CoAl_2O_4$ (**Figs. 4(a)-(c) and (f)**), nor Co_3O_4 (**Fig. 4(e)**), but it slightly matched with the peak shape of $Co(OH)_2$ (**Fig. 4(d)**). $CoAl_2O_4$ and Co_3O_4 showed completely different peak shape and the edge energy in the Co K-edge XANES (**Figs. 4(c) and (e)**). The Co K-edge XANES spectrum of 0.98_Co_3AlO_x@Al_2O_3 (**Fig. 4(g)**) appeared like the peak shape and edge energy of Co_3O_4 (**Fig. 4(e)**). The $CoAl_2O_4$ was not found in the both XRD profile and Co K-edge XANES spectrum of 0.98_Co_3AlO_x@Al_2O_3 due to the low calcination temperature at 573 K.

3.2 Oxidative dehydrogenation of 1-phenyl ethanol

The catalytic activity of prepared Co_3AlO@Al_2O_3 catalysts in oxidative dehydrogenation of 1-phenyl ethanol (**1**) was investigated using molecular oxygen as a sole oxidant (**Table 1**). All the reactions gave selectivity of higher than 99% towards acetophenone (**2**). The blank reaction was conducted in the absence of catalyst for the oxidative dehydrogenation of **1**, resulting in the very poor **2** yield (4%) (**entry 1**). The unsupported Co_3AlO catalyst, which included excess Co amount in 0.05 g, exhibited excellent **2** yield (89%) with the turnover number (TON) value based on the cobalt amount is 1.9 (**entry 3**). By supporting CO_3^{2-}/Co_3Al LDH on the surface of Al_2O_3 followed by the calcination at 573 K, the series of Co_3AlO_x@Al_2O_3 performed the oxidative dehydrogenation of **1** with the gradual decrease in the yield of **2** as the cobalt loading amounts decreased, while the TON values increased (**entries 4-6**). The support, Al_2O_3, could obtaine only 10% of **2** under the same reaction condition (**entry 2**). It suggested that Co_3O_4 that consisted in the Co_3AlO_x@Al_2O_3 matrix acted as a catalytically active site for this oxidative alcohol dehydrogenation. Different methods on supporting cobalt species to the surface of Al_2O_3 were performed and the catalytic activity was compared with the 0.98_Co_3AlO_x@Al_2O_3 derived from LDH precursor supported on Al_2O_3. Physical mixture of the metal oxide and the support material is the easiest way to produce the supported materials. In recent years, impregnation method has been widely applied to synthesis supported catalyst. As shown in **Table 1**, 0.98_Co_3AlO_x@Al_2O_3 catalyst outperformed other supported catalysts prepared using impregnation method (0.98_Co@Al_2O_3_Imp) and the physical mixture (Co_3O_4+Al_2O_3) (**entries 6, 8 and 9**). The crystallite sizes calculated from Co_3O_4(311) diffraction in the 0.98_Co@Al_2O_3 and Co_3O_4+Al_2O_3 were approximately 6.31 and 56.92 nm, respectively. It should be noted that the Co_3O_4 nanoparticles, obtained from the LDH precursor supported on Al_2O_3, exhibited higher catalytic performance compared to other Co-based support catalysts which related to the high dispersion of Co_3O_4 on Al_2O_3 surface. The highest TON value was achieved after stretching the reaction for 24 h (**entry 7**).

Table 1. Aerobic alcohol oxidation over cobalt based catalyst.[a]

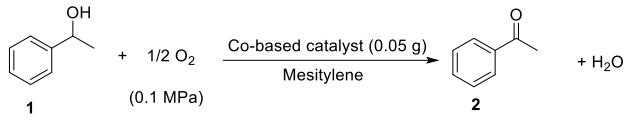

Entry	Catalyst	Co[b] (mmol/g)	Yield[c] (%)	TON[d] (-)
1	-	-	4	-
2	Al_2O_3	-	10	-
3	Co_3AlO	9.33	89	1.9
4	2.87_Co_3AlO_x@Al_2O_3	2.87	51	3.6
5	1.59_Co_3AlO_x@Al_2O_3	1.59	34	4.3
6	0.98_Co_3AlO_x@Al_2O_3	0.98	29	5.9
7[e]	0.98_Co_3AlO_x@Al_2O_3	0.98	52	10.6
8	0.98_Co@Al_2O_3_Imp	0.98	12	2.4
9[f]	Co_3O_4 + Al_2O_3	0.48	7	2.9

[a] Catalyst (0.05 g), 1-phenyl ethanol (**1**) (1 mmol), mesitylene (3 mL), O_2 (0.1 MPa), 433 K, 2 h. [b] Loading amount, confirmed by AAS. [c] Determined by GC using an internal standard technique. [d] Based on Co loading amount. [e] Reaction time for 24 h. [f] Physical mixture of 0.002 g of Co_3O_4 (Co: 0.024 mmol) and 0.048 g of Al_2O_3.

Our synthesized 0.98_Co_3AlO_x@Al_2O_3 catalyst, which was obtained by the calcination of 0.91_CO_3^{2-}/Co_3Al LDH@Al_2O_3 at 573 K, showed the TON of 10.6 based on Co amount. These calcination temperature or TON value was superior to those in previous reports: Co/Al_2O_3 (TON = 14.7, calcination temperature = 723 K)[31], Co_3O_4/MnO_2 (TON = 3.9, calcination temperature = 623 K)[32], and Co/SBA-15 (TON = 1.4, calcination temperature = 973 K)[33].

To conduct the stability test of catalyst, the recovered catalyst was collected. After catalytic reaction (**entry 6**), solid 0.98_Co_3AlO_x@Al_2O_3 catalyst was filtered from the reaction mixture, was washed using acetone several times and dried under vacuum to obtain recovered 0.98_Co_3AlO_x@Al_2O_3. A slight decrease in the catalytic performance was observed. The 1st cycle of recovered 0.98_Co_3AlO_x@Al_2O_3 transformed 21% of **1** into **2** with selectivity of higher than 99% towards **2**. Treating the recovered 0.98_Co_3AlO_x@Al_2O_3 catalyst in calcination at 573 K for 2 h under air, however, the catalytic activity was like that of the untreated recovered catalyst. This result suggested that regeneration of catalytically active site was failed via recalcination. The XRD profiles of the recovered 0.98_Co_3AlO_x@Al_2O_3 catalyst compared with the fresh one were displayed in **Fig. 5**. No change of the peak profile was notably observed between them indicating that Co_3O_4 was the main cobalt species in the catalyst matrix of the recovered catalyst as same as the fresh catalyst. The Co K-edge XANES was conducted to further investigate the change of cobalt species in the recovered catalyst. The peak shape and the edge energy of recovered

0.98_Co_3AlO_x@Al_2O_3 catalyst clearly resemble those of Co_3O_4 each other as the fresh 0.98_Co_3AlO_x@Al_2O_3 (**Figs. 4 (e, g-h)**). The oxidation state of the recovered catalyst, confirmed by the edge energy in Co K-edge XANES, did not change after the aerobic oxidation of **1**. Although no change in Co K-edge XANES spectrum was obseved, it can be speculated that partially and irreversible reduction of Co species accompanied with aggregation may take place during the catalytic reaction.

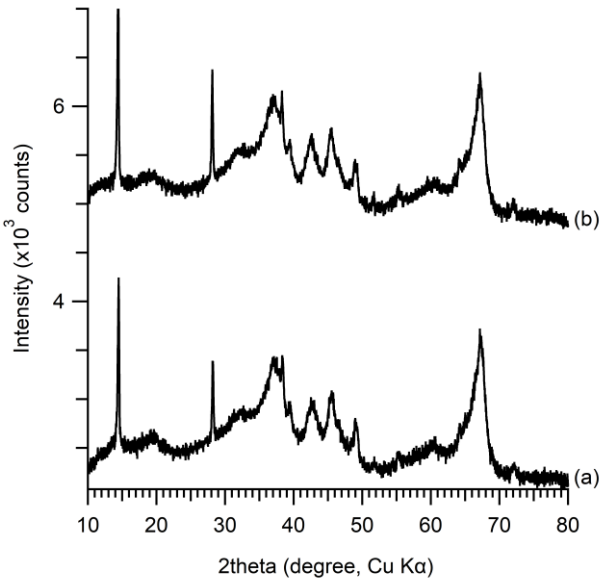

Fig. 5 XRD profiles for (a) fresh 0.98_Co_3AlO_x@Al_2O_3 and (b) recovered 0.98_Co_3AlO_x@Al_2O_3 catalyst.

4. Conclusions

In this work, the carbonate-intercalated Co^{2+}-Al^{3+} layered double hydroxide (CO_3^{2-}/Co_3Al LDH) as a nanosized precursor was carefully formed on the Al_2O_3 through a direct coprecipitation process. Subsequently, the Co_3O_4 nanocomposite, derived from the mild calcination at 573 K of the 0.91_CO_3^{2-}/Co_3Al LDH@Al_2O_3, exhibited remarkable catalytic performance in the oxidative dehydrogenation of 1-phenyl ethanol employing molecular oxygen as the oxidant. Notably, when compared to the unsupported Co_3AlO catalyst, the 0.98_Co_3AlO@Al_2O_3 catalyst demonstrated a significant enhanced performance, oxidizing 1-phenyl ethanol into acetophenone with the TON value of 10.6 which was almost 5.6 times higher than the unsupported catalyst.

Acknowledgements

T. H. received funding from JSPS KAKENHI (Grant-in-Aid for Scientific Research), Grant number 23H02000. F.Y. thanks the MEXT scholarships. Some of the experiments were carried out at a facility in the Photon Factory (KEK-PF, Proposal No. 2022G082). Synchrotron radiation X-ray diffraction experiments were performed at BL02B2, SPring-8, with approval from the Japan Synchrotron Radiation Research Institute (JASRI): 2022B1643 (T. H.), 2022A1175 (T. O.), and 2023B1759 (S. R.).

References

1) T. Baskaran, J. Christopher and A. Sakthivel, *RSC Adv.*, **5**, 98853 (2015).
2) Q. Wang and D. O'hare, *Chem. Rev.*, **112**, 4124 (2012).
3) K. Kaneda and T. Mizugaki, *Green Chem.*, **21**, 1361 (2019).
4) W. Zhou, J. Liu, J. Pan, F. Sun, M. He and Q. Chen, *Catal. Commun.*, **69**, 1 (2015).
5) M. Luo, S. Xu, Q. Gu, Z. Di, Q. Liu and Z. Zhao, *J. Colloid Interface Sci.*, **538**, 440 (2019).
6) S. Das and K. Parida, *Mater. Today Proc.*, **35**, 275 (2021).
7) M. Zubair, M. Daud, G. McKay, F. Shehzad and M. A. Al-Harthi, *Appl. Clay Sci.*, **143**, 279 (2017).
8) L. C. Santos, A. F. da Silva, P. V. dos Santos Lins, J. L. da Silva Duarte, A. H. Ide and L. Meili, *Environ. Sci. Pollut. Res.*, **27**, 5890 (2020).
9) R. M. M. Santos, V. Briois, L. Martins and C. V. Santilli, *ACS Appl. Mater. Interfaces*, **13**, 26001 (2021).
10) G. Fan, F. Li, D. G. Evans and X. Duan, *Chem. Soc. Rev.*, **43**, 7040 (2014).
11) J. Taghavimoghaddam, G. P. Knowles and A. L. Chaffee, *J. Mol. Catal. A Chem.*, **358**, 79 (2012).
12) J. J. Villora-Picó, I. Campello-Gómez, J. C. Serrano-Ruiz, M. M. Pastor-Blas, A. Sepúlveda-Escribano and E. V. Ramos-Fernández, *Catal. Sci. Technol.*, **11**, 3845 (2021).
13) W. Zhang, Y. Zhou, M. Shamzhy, S. Molitorisová, M. Opanasenko and A. Giroir-Fendler, *ACS Appl. Mater. Interfaces*, **13**, 15143 (2021).
14) D. Han, X. Ma, X. Yang, M. Xiao, H. Sun, L. Ma, X. Yu and M. Ge, *J. Colloid Interface Sci.*, **603**, 695 (2021).
15) S. Dissanayake, N. Wasalathanthri, A. Shirazi Amin, J. He, S. Poges, D. Rathnayake and S. L. Suib, *Appl. Catal. A Gen.*, **590**, 117366 (2020).
16) R. Ramos, A. F. Peixoto, B. I. Arias-Serrano, O. S. G. P. Soares, M. F. R. Pereira, D. Kubička and C. Freire, *ChemCatChem*, **12**, 1467 (2020).
17) M. H. Abdel-Aziz, M. S. Zoromba, M. Bassyouni, M. Zwawi, A. A. Alshehri and A. F. Al-Hossainy, *J. Mol. Struct.*, **1206**, 127679 (2020).
18) S. A. C. Carabineiro, A. P. C. Ribeiro, J. G. Buijnsters, M. Avalos-Borja, A. J. L. Pombeiro, J. L. Figueiredo and L. M. D. R. S. Martins, *Catal. Today*, **357**, 22 (2020).
19) F. Yu, X. Xiong, K. Huang, Y. Zhou and B. Li, *CrystEngComm*, **19**, 2126 (2017).
20) D. Ji, N. Xi, G. Li, P. Dong, H. Li, H. Li, C. Li, P. Wang and Y. Zhao, *Mol. Catal.*, **508**, 111579 (2021).
21) S. D. Kurbah, M. Asthana, I. Syiemlieh and R. A. Lal, *Appl. Organomet. Chem.*, **32**, 1 (2018).
22) A. A. Q. Ali and Z. N. Siddiqui, *Res. Chem. Intermed.*, **49**, 1085 (2023).
23) A. L. Cánepa, V. R. Elías, V. M. Vaschetti, E. V. Sabre, G. A. Eimer and S. G. Casuscelli, *Appl. Catal. A Gen.*, **545**, 72 (2017).
24) M. Li, X. Fu, L. Peng, L. Bai, S. Wu, Q. Kan and J. Guan, *ChemistrySelect*, **2**, 9486 (2017).

25) W. Zhang, Z. Xiao, J. Wang, W. Fu, R. Tan and D. Yin, *ChemCatChem*, **11**, 1779 (2019).
26) C. Bai, A. Li, X. Yao, H. Liu and Y. Li, *Green Chem.*, **18**, 1061 (2016).
27) Q. Zhang, X. Fu, Q. Kan and J. Guan, *Ind. Eng. Chem. Res.*, **58**, 4774 (2019).
28) Q. Wang, L. Chen, S. Guan, X. Zhang, B. Wang, X. Cao, Z. Yu, Y. He, D. G. Evans, J. Feng and D. Li, *ACS Catal.*, **8**, 3104 (2018).
29) A. Jha and C. V. Rode, *New J. Chem.*, **37**, 2669 (2013).
30) J. Zhu, Y. Zhao, D. Tang, Z. Zhao and S. A. C. Carabineiro, *J. Catal.*, **340**, 41 (2016).
31) V. G. Reddy, D. Jampaiah, A. Chalkidis, Y. M. Sabri, E. L. H. Mayes and S. K. Bhargava, *Catal. Commun.*, **130**, 105763 (2019).
32) J. Albadi, A. Alihosseinzadeh, M. Jalali., M. Shahrezaei and A. Mansournezhad, *Mol. Catal.*, **440**, 133 (2017).
33) X. Yang, S. Wu, L. Peng, J. Hu, X. Wang, X. Fu, Q. Huo and J. Guan, *RSC Adv.*, **5**, 102508 (2015).
34) F. Yusniyanti, T. Hara, K. Makishima, E. Kurniawan, T. Fujimura, R. Sasai, C. Moriyoshi, S. Kawaguchi, Y. Permana and N. Ichikuni, *Chem. Asian J.*, **18**, e202300727 (2023).
35) K. Wu, Q. Ye, L. Wang, F. Meng and H. Dai, *J. CO_2 Util.*, **60**, 101982 (2022).
36) F. Yusniyanti, T. Hara and N. Ichikuni, *J. Ion Exchange*, **33**, 105 (2022).
37) B. Ravel and M. Newville, *J. Synchrotron Radiat.*, **12**, 537 (2005).
38) F. Zhang, B. Lu and P. Sun, *Int. J. Hydrogen Energy*, **45**, 16183 (2020).
39) J. He, Z. Yang, L. Zhang, Y. Li and L. Pan, *Int. J. Hydrogen Energy*, **42**, 9930 (2017).
40) E. Kurniawan, T. Hara, Y. Permana, N. Ichikuni and S. Shimazu, *Chem. Lett.*, 51, 334 (2022).
41) E. Kurniawan, T. Hara, Y. Permana, T. Kojima, N. Ichikuni and S. Shimazu, *Bull. Chem. Soc. Jpn.*, 95, 121 (2022).
42) T. Onfroy, W.-C. Li, F. Schüth and H. Knözinger, *Top. Catal.*, **54**, 390 (2011).
43) Q. Zhao, Y. Ge, K. Fu, N. Ji, C. Song and Q. Liu, *Chemosphere*, **204**, 257 (2018).
44) A. Shimamura, M. I. Jones and J. B. Metson, *J. Solid State Chem.*, **316**, 123567 (2022).